International Journal of GEOMATE, Dec., 2017, Vol. 13, Issue 40, pp. 183-188
Special Issue on Science, Engineering & Environment, ISSN: 2186-2990, Japan
DOI: https://doi.org/10.21660/2017.40.171130

MICROSTRIP COUPLED LINE BANDPASS FILTER WITH RADIAL STUBS FOR NARROW-BAND APPLICATIONS

S. M. Kayser Azam, *Muhammad I. Ibrahimy, S. M. A. Motakabber and A. K. M. Zakir Hossain

Faculty of Engineering, International Islamic University Malaysia, Kuala Lumpur, Malaysia

*Corresponding Author, Received: 20 Nov. 2017, Revised: 10 Dec. 2017, Accepted: 20 Dec. 2017

ABSTRACT: The necessity of creating channels by utilizing narrow-bands in high frequency regions is a matter of concern for the next generation-oriented wireless communication systems. A microstrip bandpass filter for narrow-band applications has been proposed in this article. Two coupled line filters with tapered line resonators are loaded at the mid-points of two identical pairs of radial stubs. The scalable length of microstrip lines to extend the radial stubs provides over 536 MHz shift of the resonant frequency with a narrow-band at each perturbing step. The proposed filter has been designed on Taconic TLX-8 substrate with 0.5 *mm* thickness and its filtering parts occupy a nominal area of 131.09 mm^2 without feedlines. The fabricated filter exhibits nearly a 50 MHz pass-band at 6.428 GHz center frequency according to the measurement. Steep response of this filter entirely attenuates the out-band signal which enables it to be suitable for narrow-band applications in the higher frequency regions of C-band and ultra-wideband.

Keywords: Microstrip, Bandpass Filter, Coupled Line, Radial Stubs, Narrow-band

1. INTRODUCTION

Modern radio frequency (RF) based communication systems require bandpass filter (BPF) for narrow-band applications to avoid signal interference and provide specified channel [1]. In fact, designing BPFs with narrow bandwidth to create multi-channels is an unavoidable demand in RF filter development. Therefore, research on narrow pass-band by completely rejecting the out-band signals within a certain frequency range is rapidly increasing nowadays for different commercial, security and mobile applications. However, channel occupancy in ISM bands and WLAN applications according to IEEE 802.11 standards urges to utilize other bands for future purposes [2], [3]. In terms of the definitions given by FCC and IEEE, the rapid growth of radio frequency identification and item tracking systems inspire the RF researchers to use the higher frequency regions (above 6 GHz) in ultra-wideband (3.1 GHz to 10.6 GHz) and C-band (4 GHz to 8 GHz) [4].

In recent, researchers have proposed many techniques of designing the microstrip BPF for narrow-band applications. Microstrip passive resonators of different shapes and orientations are mostly incorporated with these techniques. Since microstrip passive resonators are further utilized in monolithic microwave integrated circuits (MMIC) nowadays, shape and orientation of the passive resonators are significant to reduce the electro-magnetic interference with other circuit elements in proximity [5]. Therefore, attention should be given by the designers to the compactness and symmetry of resonators. To achieve the compactness of microstrip BPF, folding technique is utilized by [6], where capacitive gap and via ground holes are realized by a hairpin-line BPF. For further compactness, a thick substrate with high dielectric permittivity is used which reduces the width of microstrip lines. Unfortunately, high dielectric permittivity results in additional losses and thick substrate reduces the electric coupling of the capacitive gaps [7]. Again, it is a challenge to realize the microstrip narrow BPF with simultaneously achieving a wideband rejection. Although defected ground structure (DGS) rejects signal over a wideband, open portions of the ground plane cause unwanted radiation which is a major drawback of DGS [8]. Meanwhile, radial stubs are loaded with microstrip narrow BPF because they have inherent wide-stopband properties [9]. A bell-shaped microstrip BPF with radial stubs is recently proposed in [3], where coupled line resonators are employed with folding and metered bending techniques. However, insertion loss of the proposed BPF in [3] is high and the passband is not compatible for creating a channel bandwidth.

To deal with these problems, two microstrip coupled line resonators are loaded with two identically designed radial stubs. Tapered transmission lines are employed as the connecting parts between coupled line ends and radial stubs. As a thin substrate of 0.5 *mm* thickness with low dielectric permittivity of 2.55, Taconic TLX-8 is utilized in this design which offers a compact filtering area of 131.09 mm^2. The designed BPF works at 6.428 GHz with a small fractional

bandwidth of 0.467% in terms of 10-dB attenuation. This allows the BPF to operate with nearly a 50 MHz passband by the entire rejection of out-band signals which is suitable for creating channels in C-band and UWB applications. The proposed BPF is scalable over a 536 MHz band of frequency simply by adjusting the length of microstrip lines through which the radial stubs are fed. Upcoming sections of this article present the constructional features of the proposed filter and analytical discussion of its results.

2. FILTER DESIGN AND SYNTHESIS

Characteristic impedance of each resonating part is the fundamental constituent of filter design. In case of a substrate with specified dielectric permittivity and height, the characteristic impedance (Z_0) of each passive resonator is found from the width of microstrip line and height of the substrate with effective dielectric constant of $\in_e$. This is well-explained in [10] by using the following expressions,

$$\in_e = \frac{\varepsilon_r+1}{2} + \frac{\varepsilon_r-1}{2}\frac{1}{\sqrt{1+12d/w}} \quad (1)$$

$$Z_0 = \frac{60}{\sqrt{\in_e}}\ln\left(\frac{8d}{w}+\frac{w}{4d}\right) \quad (2)$$

$$Z_0 = \frac{120\pi}{\sqrt{\in_e}\left[\frac{w}{d}+1.393+0.667\ln\left(\frac{w}{d}+1.444\right)\right]} \quad (3)$$

where, w denotes the width of a microstrip line, and d is the substrate height with dielectric permittivity of ε_r. When $w/d \leq 1$, characteristic impedance is found by using Eq. (2). Likewise, Eq. (3) is utilized to determine the characteristic impedance in case of $w/d \geq 1$. Therefore, prior to design the filter, Taconic TLX-8 is selected as the substrate material. This substrate has comparatively thinner dielectric height (0.5 *mm*) and lower relative dielectric permittivity ($\varepsilon_r = 2.55$) than other conventional substrates. Both the ground plane and microstrip lines have copper as perfect electric conductor (PEC) with 0.035 *mm* thickness. Consequently, low dielectric loss of the filtering parts and high electric coupling between the microstrip coupled lines are primarily ensured. The proposed filter is designed at a center frequency of 6.48 GHz. The schematic layout in Fig.1(a) illustrates the overall construction of the proposed BPF. In fact, the filtering parts of the BPF are supported by two microstrip feedlines at both ends which provide fine matching with the connecting ports. These feedlines are simply constructed by $\lambda/4$ microstrip transmission lines.

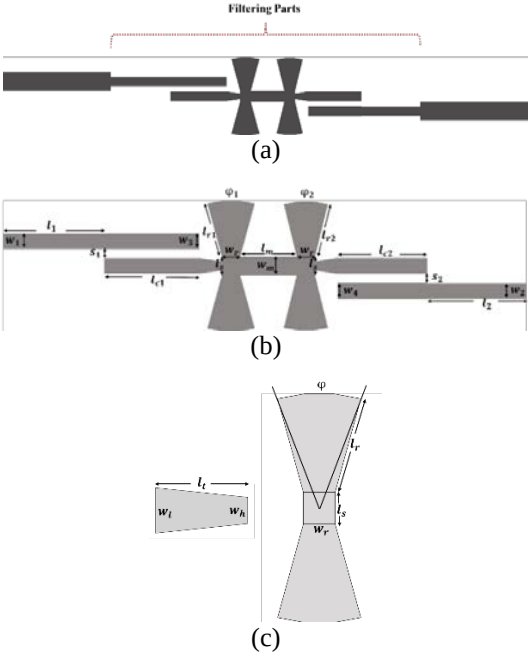

Fig.1 Proposed BPF construction (a) schematic layout with feedlines (b) dimensional presentation of the filtering parts (c) tapered line, radial stub and scalable microstrip line

On the other hand, the filtering parts, which are the core section of proposed BPF, symmetrically consist of two microstrip lines, coupled line resonators, tapered lines and identical pairs of radial stubs. Symmetry is provided by the connecting line between the two identical pairs of radial stubs. The dimensional presentation of the filtering parts is given in Fig.1(b), where the scalable length of the microstrip lines is denoted as l_s. Width of these microstrip lines is same as the width of the radial stubs. This is well-illustrated in Fig.1(c) for better understanding. Furthermore, the low impedance sides (w_l) of the tapered line resonators are constructed with the same width of coupled line resonators, while the high impedance sides are connected to the mid-points of the scalable length (l_s) of microstrip lines to feed the pairs of radial stubs.

An equivalent circuit model is constructed in Fig.2 where each microstrip line is replaced with their corresponding characteristic impedance and electrical length. For the coupled line resonators, the gap-coupled capacitances are presented by their lumped equivalent models as C_{g1} and C_{g2} respectively. By this manner, electric coupling co-efficient is also replaced for both coupled line resonators. On the other hand, tapered microstrip lines and radial stubs are replaced by lumped

elements without loss components to provide simplicity in the equivalent model of proposed filter.

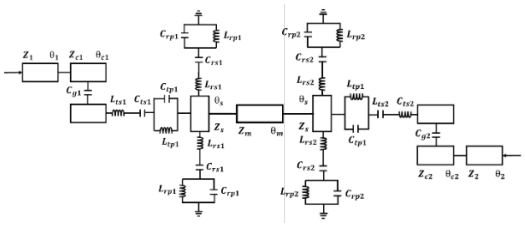

Fig.2 Lossless equivalent circuit model of the proposed filter

Unlike microstrip radial stub with small radius, the equivalent series and parallel LC-tanks of the microstrip radial stub with small angle but large radius are significant in filter analysis [11]. In addition, tapered microstrip line with significant length behaves like radial stubs with small angles. Therefore, all the microstrip tapered lines and radials stubs are presented by their equivalent lossless lumped elements.

In order to synthesize a mathematical model for the proposed filter, the equivalent circuit in Fig.2 is constructed with symmetry. Two identical structures are joined by a uniform microstrip line (Z_{m}, θ_{m}) at the middle of the filtering parts. For better representation, the filtering parts are labeled with numbers according to their orientation order and shape. However, for simplification, both the symmetrical and identical properties are equalized such as $Z_1 = Z_2 = Z$, $\theta_1 = \theta_2 = \theta$, $L_{rs1} = L_{rs2} = L_{rs}$, $C_{tp1} = C_{tp2} = C_{tp}$, $C_{g1} = C_{g2} = C_g$ and so on. In regards with the relationship between propagation constant and physical length of microstrip lines [1], the electrical length θ_s of scalable stubs perturbs the resonant frequency by the following equation.

$$\theta_s = \frac{\beta c}{n_s f_r \sqrt{\in_e}} \tag{4}$$

In Eq. (4), n_s is presented as the scaling factor of proposed BPF which is related to the resonant frequency (f_r), propagation constant (β) and the speed of light (c) in comparison with a medium of effective dielectric constant $\in_e$. However, the most significant part of filter synthesis is to find out its total input characteristic impedance. In order to calculate the total input impedance (Z_{in}) of the proposed narrow BPF, a mathematical model is derived from the proposed lossless equivalent circuit of the filter in terms of individual filtering parts which is simplified in Eq. (5) on the next page.

In terms of Fig.1(b), dimensions of the filtering parts are given in table 1. In the beginning of the design, the lengths (l_{c1} and l_{c2}), widths (w_3 and w_4) and capacitive gaps (s_1 and s_2) between the two sets of coupled line resonators are similarly constructed. Likewise, lengths (l_1 and l_2) and widths (w_1 and w_2) of the two connecting stubs at both ends are initially kept similar. However, in order to obtain the desired response of the entire BPF, these dimensions are optimized with minor changes in values. It is noteworthy that radial stubs mostly provide wide stop-band properties in filter design. However, two identical pairs of radial stubs with a small variation between their angles can contribute narrow-band characteristic in pass-band. Therefore, both identical pairs of radial stubs have the similar dimension apart from the slight difference between their radial angles.

Table 1 Dimensions of filtering parts

Part	Value (*mm*)	Part	Value (*mm*)	Part	Value (*mm*) (degree)
$\boldsymbol{l_1}$	4.46	$\boldsymbol{w_1}$	0.68	$\boldsymbol{l_t}$	1.00
$\boldsymbol{l_2}$	4.38	$\boldsymbol{w_2}$	0.67	$\boldsymbol{w_r}$	0.80
$\boldsymbol{l_{c1}}$	4.18	$\boldsymbol{w_3}$	0.68	$\boldsymbol{l_{r1}}$	2.44
$\boldsymbol{l_{c2}}$	3.95	$\boldsymbol{w_4}$	0.70	$\boldsymbol{\varphi_1}$	30.55
$\boldsymbol{s_1}$	0.40	$\boldsymbol{s_2}$	0.40	$\boldsymbol{l_{r2}}$	2.40
$\boldsymbol{l_m}$	2.50	$\boldsymbol{w_m}$	0.80	$\boldsymbol{\varphi_2}$	27.70
$\boldsymbol{w_l}$	0.40	$\boldsymbol{w_h}$	0.68	$\boldsymbol{l_s}$	0.80

According to dimensions given the in table 1, a prototype of the proposed BPF is fabricated on Taconic TLX-8 substrate by the conventional etching process. Fig.3 shows the fabricated prototype of the designed filter. SMA connectors are attached with the two feedlines and ground plane by using the soldering iron for further measurement purposes.

Fig.3 Photograph of fabricated band-pass filter

Note that any dimension below 0.3 *mm* is cumbersome to fabricate by conventional etching process. Therefore, while designing the band-pass filter, all the dimensions are selected above 0.3 *mm* to avoid fabrication errors. Nevertheless, due to the limitations of conventional etching process, any deviation below 0.1 *mm* from the original dimension is considered as fabrication tolerance.

$$Z_{in} = j\left[\frac{2\left(Z_s \tan\frac{\theta_s}{2}+\frac{\omega^2 L_{rs}C_{rs}-1}{\omega C_{rs}}-\frac{\omega L_{rp}}{\omega^2 L_{rp}C_{rp}-1}\right)\left\{Z\tan\theta+Z_c\tan\theta_c-\frac{\left(\frac{1}{\omega C_g}+Z_c\cot\theta_c\right)}{Z_c}+\frac{\omega^2 L_{ts}C_{ts}-1}{\omega C_{ts}}-\frac{\omega L_{tp}}{\omega^2 L_{tp}C_{tp}-1}\right\}}{\left(Z_s \tan\frac{\theta_s}{2}+\frac{\omega^2 L_{rs}C_{rs}-1}{\omega C_{rs}}-\frac{\omega L_{rp}}{\omega^2 L_{rp}C_{rp}-1}\right)+2\left\{Z\tan\theta+Z_c\tan\theta_c-\frac{\left(\frac{1}{\omega C_g}+Z_c\cot\theta_c\right)}{Z_c}+\frac{\omega^2 L_{ts}C_{ts}-1}{\omega C_{ts}}-\frac{\omega L_{tp}}{\omega^2 L_{tp}C_{tp}-1}\right\}}+Z_m\tan\theta_m\right] \quad (5)$$

3. RESULTS AND DISCUSSION

In terms of design method and optimized dimensions described in the earlier section, the proposed BPF is designed by using Advanced Design System (ADS) simulating software. The layout is generated, and ADS electromagnetic (EM) Momentum simulation is performed on the designed filter. The simulated results which are depicted in Fig.4(a) show that the designed BPF provides nearly a 50 MHz narrow pass-band at 6.48 GHz resonant frequency.

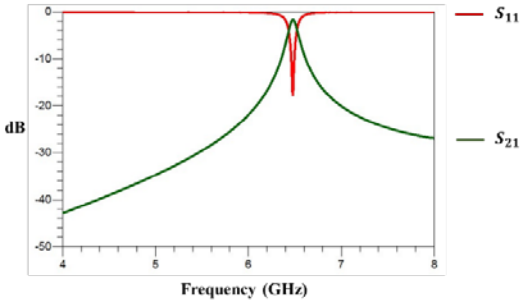

(a)

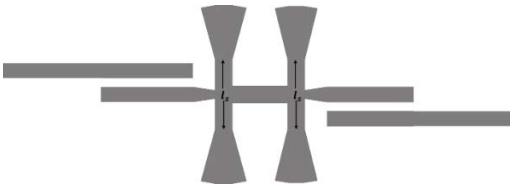

(b)

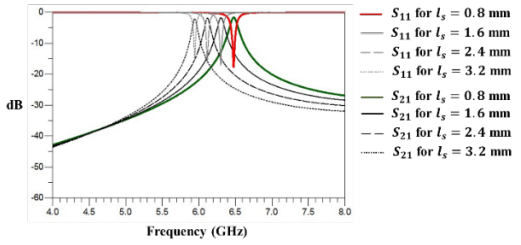

(c)

Fig.4 Simulated results and effects of extending l_s (a) simulated S_{11} and S_{21} parameters (b) extension of l_s (c) effects of extending l_s

The return loss is found below -17.95 dB, whereas the insertion loss is better than -1.68 dB. Because the filter exhibits a steep and maximally flat Butterworth response, instead of 3-dB insertion loss, the filter has a small fractional bandwidth (FBW) of 0.467% in terms of 10-dB return loss. It is remarkable to observe that the filter completely rejects the out-band signals in C-band region. Since the scaling dimension determines the frequency perturbation range [12], the scalable length (l_s) of the microstrip lines to feed the pairs of radial stubs is extended as illustrated in Fig.4(b) from $l_s = 0.8\,mm$ to $l_s = 3.2\,mm$ to obtain the desired shifts of frequency. According to the scaling effects, the resonant frequency is perturbed from 6.48 GHz to 5.944 GHz. It is remarkable to find that the bandwidth of designed filter is rather narrowed to nearly 40 MHz but in cost of 0.2 dB insertion loss during the perturbation. The perturbation is selected in such a manner so that the resonant frequency does not remain in occupied channels like intelligent transportation systems (ITS) band [2], [3]. However, the scalable length (l_s) of microstrip lines can further be extended to obtain resonant frequency for creating channels in WLAN applications. In that case, insertion loss can be increased, and entire rejection of out-band signal can be disturbed. Therefore, in terms of simulated results, it is advisable to perturb the scalable microstrip length (l_s) not more than 4 mm.

As described earlier, the proposed filter with $l_s = 0.8\,mm$ is fabricated on Taconic TLX-8 substrate through conventional etching process. Later, the fabricated filter is validated by measurements. Agilent N5230A PNA-L Network Analyzer is used to measure the frequency response of prototype narrow BPF. The measured results are shown in Fig.5(a) and Fig.5(b) which are taken from the display monitor of Agilent N5230A PNA-L Network Analyzer. According to the measured results of the prototype BPF, resonant frequency is found at 6.428 GHz. Since coupled line resonators and radial stubs are quite sensitive with their dimensions, measured frequency slightly (52 MHz) shifts from the design frequency due to the manufacturing tolerance in conventional etching process and soldering errors in SMA connectors. Observing from the display monitor of network analyzer, it is found that the fabricated filter completely rejects the out-band signal with a small fractional bandwidth (in terms of 10-dB attenuation). Although some ripples are visible in the measured results, these appear due to the aforementioned reasons. Nevertheless, the

return loss is found as − 13.236 dB which is decently below the −10 dB cut-off region. On the other hand, insertion loss is measured as −4.38 dB which is well-enough for the signal at transmitting end.

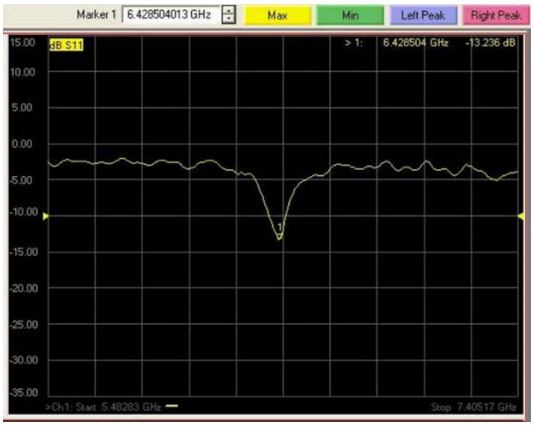

(a)

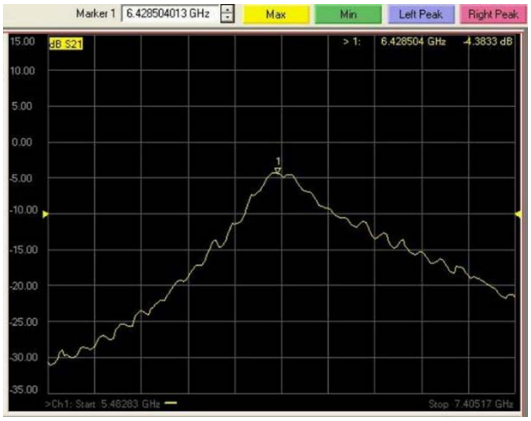

(b)

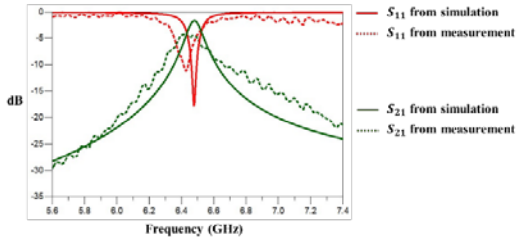

(c)

Fig.5 Measured results of prototype BPF by Agilent N5230A PNA-L Network Analyzer (a) return loss (b) insertion loss (c) comparison between results from simulation and measurement

Measurement results infer that the developed filter provides a nearly 50 MHz pass-band. This can be observed in terms of 10-dB attenuation since the frequency response is sharp and the return loss surpasses the relative 3-dB insertion loss by leaving a narrow-band to transmit the signal. In turn, such narrow-band characteristic is suitable for creating channels in the high frequency regions of C-band and UWB.

Measured results are further compared with the simulated results as illustrated in Fig.5(c). It is seen from the comparison that there has been a good agreement between the measured and simulated results. The slight deviation can be overcome by fabricating the filter through industrial process. Furthermore, in terms of physical dimensions, the proposed filter has identical, compact and symmetrical structure. Since microstrip passive filters and resonators are often implemented by MMIC technology, identical and symmetrical shape of this BPF can reduce the electromagnetic interference with nearby circuitry. Also, wide stop-band characteristic of this filter is suitable for single frequency oscillator and mixer applications. In addition, the developed narrow BPF occupies a compact area of 131.09 mm^2. In terms of resonant frequency (f_r), mostly of bandwidth (BW) and filtering area, assessment of the proposed filter by comparing with recent works for narrow-band applications is provided in Table 2 along with the performance parameters like insertion loss, return loss.

Table 2 Filter assessment

Work	f_r (GHz)	BW (MHz)	S_{21} (dB)	S_{11} (dB)	Area (mm^2)
[3]	5.75	460	-7.47	-19.31	400
[6]	3.00	74	-1.28	-27.36	218.4
[12]	2.30	120	-2.35	-25.00	82.81
This work	6.428	50	-4.38	-13.24	131.09

4. CONCLUSION

A microstrip bandpass filter is designed at 6.428 GHz resonant frequency by loading the pairs of radial stub with coupled line resonators via tapered transmission lines. Mathematical and physical synthesis of the filter are presented in this article. The designed filter allows signals for a suitable narrow-bandwidth of 50 MHz and rejects signals for all the other frequencies in C-band and UWB regions. Scalability of only one physical parameter offers the filter to be utilized for creating unoccupied channels with less than 50 MHz bandwidth over a 536 MHz perturbation range in C-band and UWB regions. This compact and thin bandpass filter is expected to be a well-competent with the growing demand of futuristic narrow-band applications in wireless communication.

5. ACKNOWLEDGEMENTS

This research has been supported by the Malaysian Ministry of Science and Technology under the eScienceFund (SF14-010-0060) and the Research Management Centre, IIUM under the project of RIGS17-006-0581.

6. REFERENCES

[1] Hong J.-S., and Lancaster M., Theory and Experiment of Novel Microstrip Slow-wave Open-loop Resonator Filters. IEEE Transactions on Microwave Theory and Techniques. Vol. 45, Issue 12, 1997, pp. 2358–2365.

[2] O'hara B., and Petrick A., IEEE 802.11 Handbook: A Designer's Companion. IEEE Standards Association, 2005, pp. 1–353.

[3] Ahmad A., and Othman A.R., Narrow Dual Bandpass Filter Using Microstrip Coupled Line with Bell Shaped Resonator, in Proc. Int. Conf. on Advances in Electrical, Electronic and Systems Engineering, 2016, pp. 550–554.

[4] Hossain A. K., Ibrahimy M. I., and Motakabber S. M., Spiral Resonator for Ultra Wide Band Chipless RFID Tag, in Proc. Int. Conf. on Computer and Communication Engineering, 2014, pp. 281–283.

[5] Azam S. M. K., Ibrahimy M. I., and Motakabber S. M. A., Reduction of Phase Noise for Inductor Based Ultra-Wide Band Voltage Controlled Oscillator, in Proc. Int. Conf. on Communication, Control, Computing and Electronics Engineering, 2017, pp. 1–4.

[6] Hasan A., Hannan A., and Nadeem A. E., Improved Microstrip Hairpinline Bandpass Filter Using Via Ground Holes and Capacitive Gap. Analog Integrated Circuits and Signal Processing. Vol. 86, Issue 2, 2016, pp. 267–274.

[7] Cao Y., Groves R.A., Huang X., Zamdmer N.D., Plouchart J.O., Wachnik R.A., King T.J. and Hu C., Frequency-independent Equivalent-circuit Model for On-chip Spiral Inductors. IEEE Journal of solid-state circuits. Vol. 38, Issue 3, 2003, pp. 419-426.

[8] Ma K., and Yeo K. S., New Ultra-Wide Stopband Low-Pass Filter Using Transformed Radial Stubs. IEEE Transactions on Microwave Theory and Techniques. Vol. 59, Issue 3, 2011, pp. 604–611.

[9] Giannini F., Sorrentino R., and Vrba J., Planar Circuit Analysis of Microstrip Radial Stub (Short Paper). IEEE Transactions on Microwave Theory and Techniques. Vol. 32, Issue 12, 1984, pp. 1652–1655.

[10] Pozar D. M., Microwave Engineering. John Wiley & Sons, 2009, pp. 148–298.

[11] Xu J., Wu W., Kang W., and Miao C., Compact UWB Bandpass Filter with a Notched Band Using Radial Stub Loaded Resonator. IEEE Microwave and Wireless Components Letters. Vol. 22, Issue 7, 2012, pp.351–353.

[12] Esfeh B.K., Ismail A., Raja Abdullah R.S.A., Adam H., and Alhawari A.R.H., Compact Narrowband Bandpass Filter Using Dual-mode Octagonal Meandered Loop Resonator for WiMAX Application. Progress In Electromagnetics Research B. Vol. 16, 2009, pp.277–290.